Design and Implementation of Classical Linear PI Controller for Fundamental Negative Output Super Lift Luo Converter

[1]R.Thamaraiselvi, [2]J.Baskaran

[1] Department of Electrical and Electronic Engineering, Anna University-Villupuram Campus, Tamil Nadu, India
E-mail: r.thamaraiselvi75@gmail.com
[2]Department of Electrical and Electronic Engineering, Adhiparasakthi College of Engineering, Tamil Nadu, India
E-mail: baskil@rediffmail.com

Abstract: This article study on a design and implementation classical linear Proportional-Integral (PI) controller for Fundamental Negative Output Super Lift Luo Converter (FNOSLLC) worked in Continuous Conduction Mode (CCM). The FNOSLLC is one of recent DC-DC converter that converts from positive DC source voltage to negative DC load voltage. The dynamic characteristic of this converter is poor performance due to non-linear nature of FNOSLLC. So as to get better dynamic performance of FNOSLLC for both the static and the dynamic specifications, a classical linear PI controller is designed. The parameters value of the PI controller is determined with help of Ziegler-Nichols tuning method. The values of PI controller setting are obtained with state-space average modeling of FNOSLLC. The computer simulation of FNOSLLC using designed control model is implemented in MATLAB/Simulink. The static and dynamic performances of the FNOSLLC are tested at various regions. The complete simulation results verify the achieve of the parameters value of PI controller on the static and the dynamic characteristics of the FNOSLLC, which is applicable for common solar cell, computer power supplies in central processing unit, mobile phones, I-pad, and physiotherapy medical equipments.

KEYWORDS: DC-DC converter, Negative Output Elementary Super Lift Luo Converter, State-Space Average Method, PI Controller.

1.

2. INTRODUCTION

DC-DC conversion technology has been developing very rapidly, and DC-DC converters have been widely used in industrial applications such as dc motor drives, computer systems and communication equipments. DC-DC converters that convert the unregulated DC input voltage into regulated DC output voltage. Nowadays, all the modern power electronics systems need high quality, simple, lightweight, cheap, highly reliable and efficient power supplies. To regulate the output voltage of DC-DC converters irrespective of load variations and line disturbances, it is necessary to operate the converters in closed loop mode. Conventionally, classical PID controllers are used for the control of DC-DC power converters has resulted in past [1-3]. The simple models of power converters are usually found from state-space averaging and linearization techniques, these models may then be used for classical control design in [4-5].

The FNOSLLC is a new series of DC-DC converters possessing high-voltage transfer gain, high power density, high efficiency, reduced ripple voltage and current [6-7]. These converters are widely used in computer peripheral equipment, industrial applications and switch mode power supply, especially for high voltage-voltage projects. The super-lift technique considerably increases the voltage transfer stage-by-stage gain in geometric progression [7-8]. Control for them needs to be study for application of these good topologies [6].

Therefore in this article, we study an output voltage regulation for FNOSLLC operated in CCM using PI controller. The state-space average model for FNOSLLC is derived at first and PI controller is designed. The performances of the controller in terms of robustness and dynamic response will be improved by proper selection of the controller parameters value. In section 2, we will present the operation and mathematical model of FNOSLLC. The design of PI controller for FNOSLLC is presented in section 3. Simulation results of system at various regions are discussed in section 4. The conclusions and future work of system is discussed in section 5.

3. OPERATION AND MATHEMATICAL MODEL OF FNOSLLC

Fig. 1 shows the circuit of FNOSLLC. It consists of includes D.C input supply voltage V_{in}, capacitors C_1 and C_2, inductor L_1, power switch (n-channel mosfet) S, freewheeling diodes D_1 and D_2 and load resistance R. In the description of the converter operation, it is assumed that all the components are ideal and also the FNOSLLC operates in a CCM. Figs. 2 and 3 shows the modes of operation of the FNOSLLC [6].

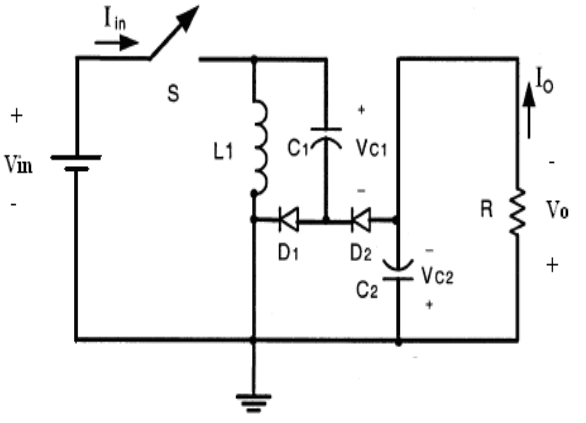

Fig. 1. The FNOSLLC circuit.

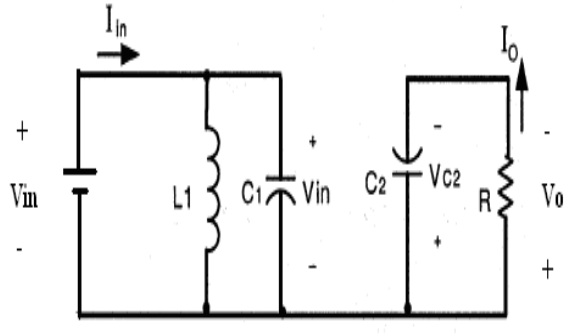

Fig. 2. Mode 1 operation.

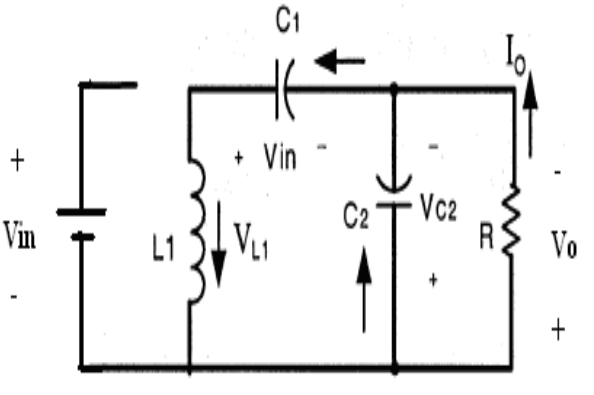

Fig. 3. Mode 2 operation.

During the on-time period of switch S the voltage across the capacitor C_1 is charged to V_{in} and the current i_{L1} flowing through the inductor L_1 increases with slope V_{in} / L_1 as shown in Fig. 2. Decreases with slope - (V_o - 2 V_{in}) / L_1 during the off-time period of switch S as shown in Fig. 3. Therefore, the ripple of the inductor current i_{L1}

$$\Delta_{iL1}=\frac{V_{in}}{L_1}dT=\frac{V_O-V_{in}}{L_1}(1-d)T \tag{1}$$

The voltage transfer gain is

$$G=\frac{V_O}{V_{in}}=\frac{2-d}{1-d}-1 \tag{2}$$

In steady state, the average charges across capacitor C_2 in a period should be zero. We have the following relations:

$$dT\, i_{C2-on}=(1-d)Ti_{C2-off} \tag{3}$$

$$i_{C2-on}=I_o \tag{4}$$

The variation ratio of inductor current i_{L1} is

$$\xi=\frac{\Delta_{iL1/2}}{i_{L1}}=\frac{d(1-d)TV_{in}}{2L_1I_o}=\frac{d(1-d)}{G_1}\frac{R}{2fL_1} \tag{5}$$

The ripple voltage of output voltage V_o is

$$\Delta_{vo}=\frac{\Delta Q}{C_2}=\frac{I_o(1-d)T}{C_2}=\frac{(1-d)}{fC_2}\frac{V_o}{R} \tag{6}$$

Therefore, the variation ratio of output voltage V_o is

$$\xi=\frac{\Delta_{vo}/2}{V_o}=\frac{(1-d)}{2RfC_2} \tag{7}$$

2.1 State-space average mathematical model of FNOSLLC

The state variables of FNOSLLC υ_1, υ_2 and υ_3 are chosen as the inductor current i_{L1}, the capacitor voltage V_{C1} and the capacitor voltage V_{C2} respectively. In Fig. 2, when the switch is closed, the state space equation of FNOSLLC is given as

$$\begin{cases}\dot{\nu}_1=-\dfrac{V_{in}}{L_1}\\ \dot{\nu}_2=\dfrac{V_{in}}{C_1R_{in}}-\dfrac{\nu_1}{C_1}\\ \dot{\nu}_3=-\dfrac{\nu_3}{RC_2}\end{cases}$$

In Fig. 3, when the switch is open, the state space equation of FNOSLLC is given as

$$\begin{cases} \dot{\nu}_1 = -\dfrac{\nu_2}{L_1} - \dfrac{\nu_3}{L_1} \\ \dot{\nu}_2 = \dfrac{\nu_1}{C_1} \\ \dot{\nu}_3 = \dfrac{\nu_1}{C_2} - \dfrac{\nu_3}{RC_2} \end{cases}$$

The state-space modeling [4-5] of the equivalent circuit of FNOSLLC with state variables i_{L1}, V_{C1} and V_{C2} is given by

$$\begin{bmatrix} \frac{di_{L1}}{dt} \\ \frac{dV_{C1}}{dt} \\ \frac{dV_{C2}}{dt} \end{bmatrix} = \begin{bmatrix} 0 & -\frac{1}{L_1} & \frac{1}{L_1} \\ \frac{1}{C_1} & 0 & 0 \\ \frac{1}{C_2} & 0 & -\frac{1}{RC_2} \end{bmatrix} \begin{bmatrix} i_{L1} \\ V_{C1} \\ V_{C2} \end{bmatrix} + \begin{bmatrix} \frac{V_{C1}}{L_1} - \frac{V_{C2}}{L_1} + \frac{V_{in}}{L_1} \\ -\frac{2i_{L1}}{C_1} + \frac{V_{in}}{R_{in}C_1} \\ -\frac{i_{L1}}{C_2} \end{bmatrix} \gamma + \begin{bmatrix} -\frac{V_{in}}{L_1} \\ 0 \\ 0 \end{bmatrix} \tag{8}$$

$$\dot{\nu} = A\nu + B\gamma + C$$

Where R_{in} is internal source resistance, which is not shown in the circuit because it is very small value hence it can be neglected, γ is the status of the switches, υ and ύ are the vectors of the state variables (i_{L1}, V_{C1} , V_{C2}) and their derivatives respectively,

$$\gamma = \begin{cases} 1 \rightarrow S \rightarrow ON \\ 0 \rightarrow S \rightarrow OFF. \end{cases} \tag{9}$$

4. DESIGN OF PI CONTROLLER FOR FNOSLLC

The closed loop model of PI controller for FNOSLLC is shown in Fig. 4. The control scheme consists of only one voltage feedback. The output voltage of FNOSLLC is fed back and compared with Vo reference voltage and the error is given to the PI controller to stabilize the error and the signal obtained from the controller is the modulating signal for the pulse width modulation (PWM) scheme. Signal from the PI controller is compared with high frequency triangular carrier signal (100 kHz) to produce required pulse for the N-channel MOSFET switch to obtain the reference DC voltage at the output.

In this article, design of PI controller for the FNOSLLC is obtained by using the Ziegler-Nichols method – 1, which is (S-shaped curve technique) [9-10]. Step input is applied to the plant model of (8) and the response is the S shaped curve. By drawing the tangent to the S shaped curve at its inflection point with reference to X-axis, the time delay L and time constant T are calculated. Using Ziegler-Nichols chart [9-10], the value of the Kp and Ti calculated. The PI controller optimal setting values of Kp and Ti for FNOSLLC are obtained by finding the minimum values of integral of square of error (ISE), integral of time of square of error (ITAE) and integral of absolute of error (IAE), which is listed in **Table 1**.

Table. 1. Simulated results of minimum values of ISE, IAE, ITAE and optimal setting values of Kp and Ti

ISE	IAE	ITAE	Kp	Ti (s)
2.27	0.1635	0.0001557	0.01205	0.02803

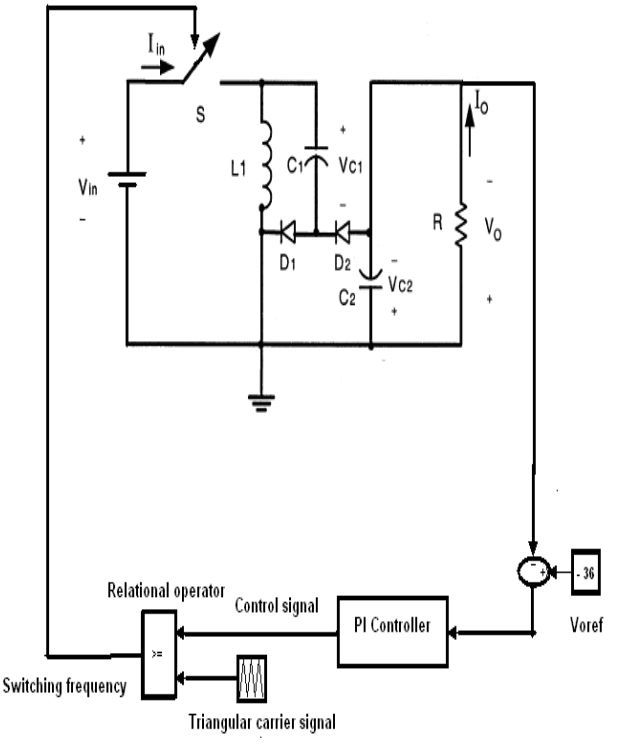

Fig. 4. Closed loop model of PI controller scheme for FNOSLLC

5. SIMULATION RESULTS

The simulation result of FNOSLLC with PI controller scheme is presented in this section. The validation of the system performance is done for five regions viz. transient region, line variations, load variations, steady state region and also components variations. Simulations have been performed on FNOSLLC circuit with parameters listed in **Table 2**. The static and dynamic performances of PI controller for FNOSLLC are evaluated in MatLab/Simulink.

Table. 2. Parameters of FNOSLLC.

Parameters name	Symbol	Value
Input Voltage	Vin	12V
Output Voltage	Vo	-36V
Inductor	L_1	100µH
Capacitors	C_1, C_2	30 µF
Nominal switching frequency	Fs	100kHz
Load resistance	R	50Ω
Output power	Po	25.92W
Input power	Pin	28.236W
Input current	Iin	2.353 A
Efficiency	η	91.79%
Average Output Current	Io	-0.72 A
Adopted value of duty ratio	d	0.66
Range of duty ratio	d	0.3 to 0.9

4.1 Transient region

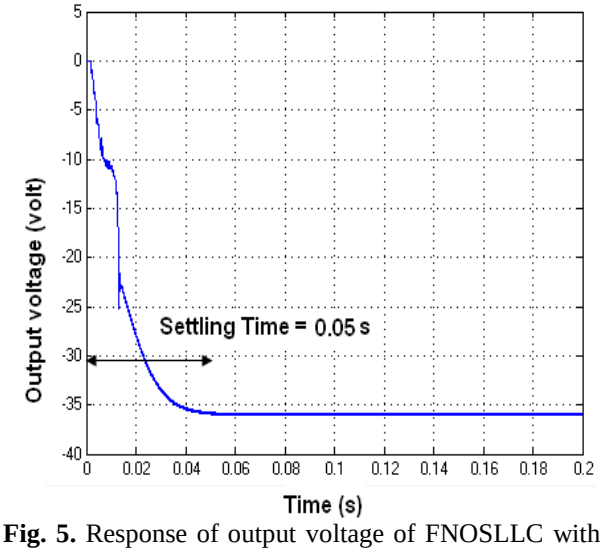

Fig. 5. Response of output voltage of FNOSLLC with PI controller in startup region.

Fig. 5 shows the dynamic behavior in the startup for output voltage of FNOSLLC with PI controller for input voltage of 12 V. It could be seen that the output voltage has a negligible overshoot and settling time of about 0.05 s with designed PI controller.

4.2 Line variations

Fig. 6 shows the response of average output voltage of FNOSLLC with PI controller for input voltage step change from 12V to 15V (+30% line variations). It could be seen that the output voltage of FNOSLLC has maximum overshoot of -12V and settling time of 0.04s with designed PI controller.

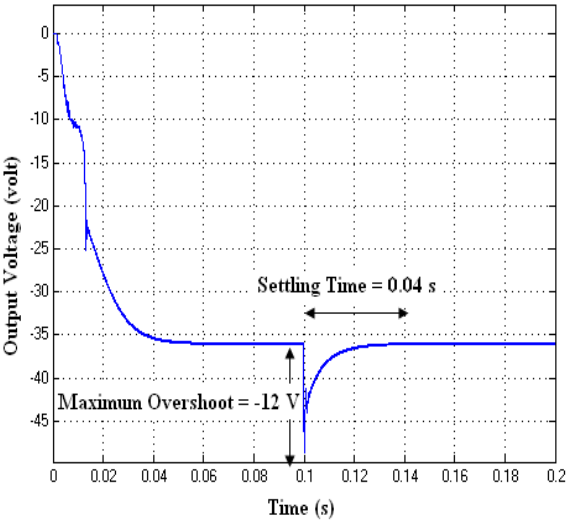

Fig. 6. Response of output voltage of FNOSLLC with PI controller for input step change from 12V to 15V.

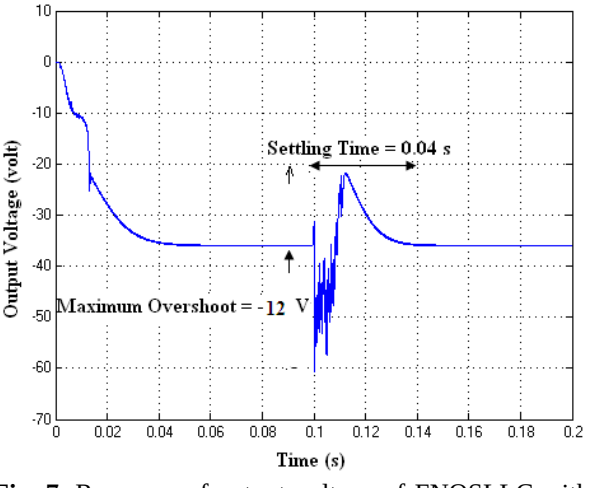

Fig. 7. Response of output voltage of FNOSLLC with PI controller for input step change from 12V to 9V.

Fig. 7 shows the response of average output voltage of FNOSLLC with PI controller for input voltage step change from 12V to 9V (-30% line variations). It can be observed that the output voltage of FNOSLLC has maximum overshoot of -12V and settling time of 0.04s with designed PI controller.

4.3 Load variation

Fig. 8 shows the response of output voltage of FNOSLLC with PI controller for load step change 50Ω to 60Ω (+20% load variations). It could be seen that the output voltage of FNOSLLC small overshoot of -3.5V and smaller settling time of 0.04s with designed PI controller.

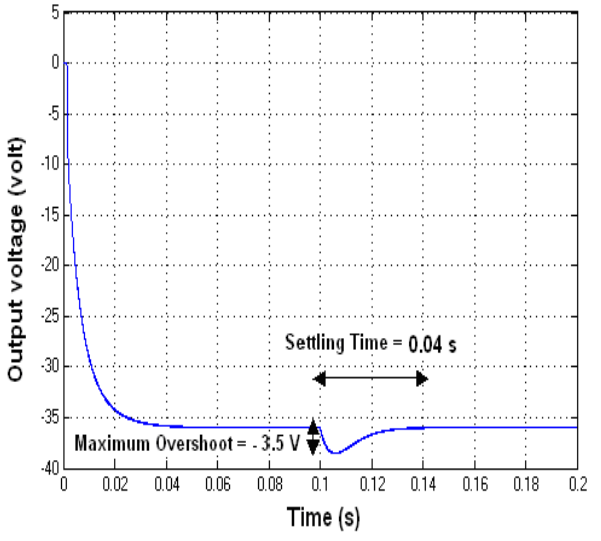

Fig. 8. Response of output voltage of FNOSLLC with PI controller when load value takes a step changes from 50Ω to 60Ω.

4.4 Steady State region

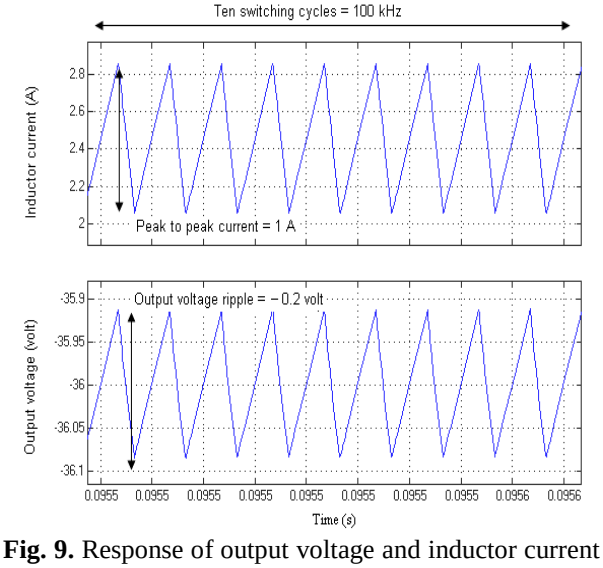

Fig. 9. Response of output voltage and inductor current FNOSLLC with PI controller in steady state region.

Fig. 9 shows the instantaneous output voltage and current of the inductor current of FNOSLLC with PI controller in the steady state. It is evident from the figure that the output voltage ripple is very small about - 0.2V and the peak-to-peak inductor current is 1A for the average switching frequency (100 kHz) closer to theoretical designed value listed in **Table 2**.

4.5 Circuit components variation

Fig. 10 shows the output voltage of FNOSLLC with PI controller for inductor variation from 100µH to 500µH. It can be found that the change does not influence the converter behaviors due to designed PI controller. An interesting result is illustrated in Fig. 11. It shows the output voltage response of FNOSLLC with PI controller for the variation in capacitor values from 30µF to 100µF. It can be seen that the PI controller is very successful in suppressing effect of capacitance variation except that a slightly output voltage ripples.

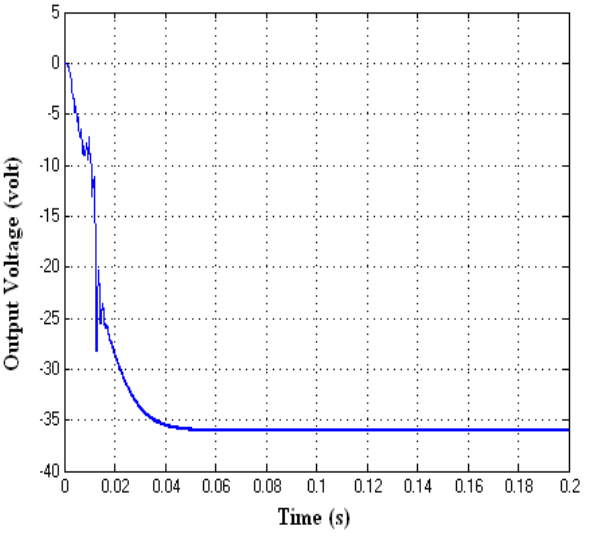

Fig.10. Output voltage of FNOSLLC with PI controller when inductor variation from 100 µH to 500 µH.

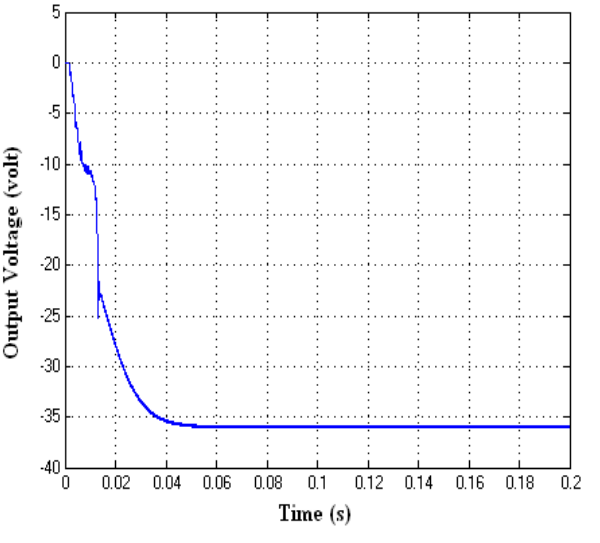

Fig.11. Output voltage of FNOSLLC with PI controller when capacitors variation from 30 µF to100 µF.

In Fig. 12 show the average input current and average output current FNOSLLC with PI controller. It is showed that the average input current is 2.456 A and average output current is - 0.72A, which is closer to theoretical value in **Table 2**. Using simulation analysis FNOSLLC with PI controller computes that the input, output power and efficiency values are 29.472W,

25.92W and 87.94% respectively, which is closer to the calculated theoretical value listed in **Table 2.**

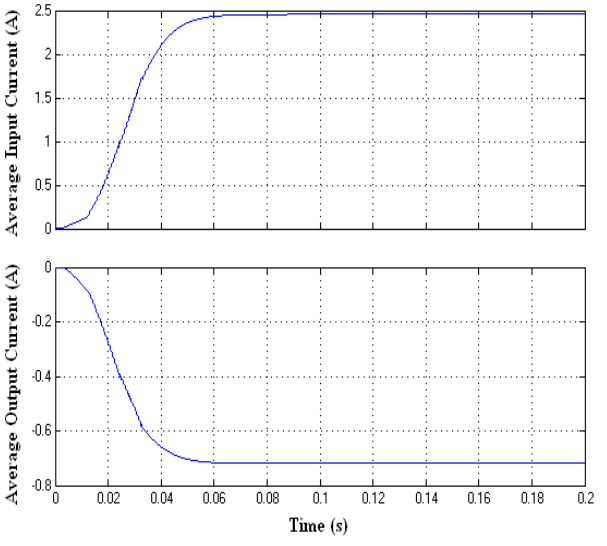

Fig. 12. Average input current and output current of NOESSLC with PI controller.

6. CONCLUSIONS

The design and output voltage regulation of classical linear PI controller for FNOSLLC operated in CCM has been successfully demonstrated in MATLAB/Simulink software platform. A classical linear PI controller over the output voltage has been used for the control. The PI controller is designed using state-space average method in this article and also the influence of the controller parameters on the performances of the system was studied. The effect of proper selected controller parameters of PI controlled FNOSLLC operated in CCM resulted in fast dynamic response and excellent static and transient responses. It is, therefore, feasible for common DC-DC conversion purpose, computer power supplies and medical equipments etc. Further research may focus to the study of the system, and on the stability of the controller-observer in closed loop operation.

REFERENCES

[1] S. Arulselvi, G. Uma and M. Chidambaram,; **"Design of PID controller for boost converter with RHS zero"**, 4th International Power Electronics and Motion Control Conference (IPEMC 2004), 14-16 august 2004, China.

[2] L. Guo, J.Y. Hung and R. M. Nelms; **"Design and implemenation of a digital PID controller for a buck converter"**, Proceedings of the 36th Intersociety Energy Conversion Engineering Conference, July/August (2001), Vol. 1, pp. 187-192.

[3] H. Mingzhi and X. Jianping,; **"Nonlinear PID in Digital Controlled Buck Converters"**, Applied power electronics conference APEC 2007, 25 Feb-1 March (2007), Anahein CA USA, pp. 1461-1465.

[4] A.J. Foreyth and S.V. Mollov,; **"Modeling and control of Dc-Dc converters"**, IEEE Power Engineering Journal, Vol. 12 no. 5, (1998), pp 229-236.

[5] Mahdavi, A. Emadi, H.A. Toliyat,; **"Application of State Space Averaging Method to Sliding Mode Control of PWM DCDC Converters"**, IEEE Industry Applications Society Annual Meeting New Orleans**,** Louisiana, October 5-9, (1997), pp. 820-827.

[6] F.L.Luo and H.Ye,; **"Negative output super lift converters"**, IEEE Transaction on power electronics, Vol.18, No. 5, September (2003), pp. 1113-1121.

[7] F.L.Luo and H.Ye,; **"Analysis of Luo converters"**, IEE Proc.-Electr. Power Appl., Vol.151, No.5, pp.590-606, September (2004)

[8] Fang Lin Luo and Hong Ye,; **"Advanced Dc/DC Converters",** CRC Press, London.

[9] P. Comines and N. Munro,; "**PID controllers: recent tuning methods and design to specification"**, in *IEEE Proc. Control Theory Application*, vol.149, no.1, pp.46-53, Jan 2002.

[10] Katsuhiko Ogata,; **"Modern Control Engineering"**, Published by Prentice – Hall of India Private Limited, New Delhi, Third Edition.